MICROSTRUCTURAL, MECHANICAL AND CORROSION BEHAVIOUR OF B_4C/BN-REINFORCED Al7075 MATRIX HYBRID COMPOSITES

N. Ramadoss
Department of Mechanical Engineering, ARM College of Engineering and Technology, Maraimalai Nagar, Chengalpattu, Chennai, Tamilnadu 603 209, India

K. Pazhanivel
Department of Mechanical Engineering, ARS College of Engineering, Maraimalai Nagar, Chennai 603 209, India

A. Ganeshkumar
Department of Mechanical Engineering, Thiruvalluvar College of Engineering and Technology, Vandavasi 604505, India

M. Arivanandhan
Centre for Nanoscience and Technology, Anna University, Chennai 600025, India

https://doi.org/10.1007/s40962-022-00791-z

Abstract

In this work, significant attention has been given to improve the mechanical and corrosion behaviour of aluminium hybrid metal matrix composites (AHMMCs) of Al7075 with boron carbide (B_4C) and boron nitride (BN) as reinforcement particles. The AHMMCs with various weight % (3%, 6%, and 9% by weight) of B_4C and fixed weight percentage (3%) of BN particulates were synthesized using the stirring-squeeze cast method. The microstructure images of composites show the grains enrichments. The XRD and SEM studies confirm the formation of intermetallic materials as a secondary phase like Al_3BC, AlB_{12} and AlN in the AHMMCs and better distribution of the reinforcement particles. The improvements in the hardness, tensile, compressive, wear and corrosion resistance of composites were achieved. The enriched grains and intermetallic materials play a predominant role in improving the strength of the hybrid composites. The SEM micrographs of corroded surfaces of the composite reveal that the formation of protective layer supports the higher corrosion resistance of the composites. The study reveals that the B_4C- and BN-reinforced aluminium matrix hybrid composites could be a potential candidate for automotive and marine applications.

Keywords: *hybrid metal matrix composites, boron carbide (B_4C), boron nitride (BN), corrosion, wear, hardness, mechanical properties*

Introduction

Metal matrix composites (MMCs) are frequently used materials in industrial applications due to their advantages over polymer matrix composites (PMCs) and ceramics matrix composites (CMCs). MMCs exhibit mechanical and physical properties superior to that of PMCs. Aluminium is one of the most popular and commonly used metals because of its simplicity in handling, lightweight with good corrosion resistance, high strength and low production and manufacturing cost. Aluminium-based MMCs are widely used in automotive and aerospace applications, since their unique properties like greater strength, reduced density, controlled thermal expansion and better wear resistance.[1] In aluminium-based MMCs, base constituent is an aluminium alloy (i.e. Al–Si, Al–Cu, Al–Si–Mg), which forms percolating network and is termed as matrix phase. The other constituent is embedded in this aluminium/aluminium alloy matrix and serves as reinforcement, which is

Received: 09 January 2022 / Accepted: 04 March 2022 /
Published online: 7 April 2022

usually non-metallic and common ceramic such as SiC, Al_2O_3, C, B, B_4C, AlN and BN. The properties like tensile strength, compressive strength, impact strength, hardness, wear resistance and corrosion resistance were found to be positively improved with reinforcement addition thereby making them a suitable material than the unreinforced base aluminium alloy. It is also found that B_4C reinforcements exhibit higher hardness than TiC, TiB_2, SiC, Al_2O_3 and Gr.[2] The enhancement of mechanical properties was achieved for Al7075 composites attained by reinforcing micro- and nanoparticles of Al_2O_3 and B_4C.[3] The demand for aluminium hybrid composite has been increased due to the enhanced processing methods, reliable production cost and desired high mechanical and tribological properties. The structural and functional application of the aluminium hybrid composites and the selection of parameters for synthesizing are mostly influenced by the selection of reinforcements.[4] The addition of reinforcement particles not only increases the hardness but also the brittle nature of the composites. These restrictions can be rectified by adding secondary reinforcement to achieve further improvements in the mechanical properties of the hybrid composites.[5] Various kinds of reinforcement and co-reinforcement have been used to improve the behaviour on mechanical properties of aluminium composites for different engineering applications.[6–9] MMCs can be processed using three main methods they are, solid-state processing, liquid-state processing and in-situ processing. Fabrication techniques usually vary according to the reinforcements. However, there are various techniques such as stir casting, liquid metal infiltration, squeeze casting, spray decomposition and powdered metallurgy[10,11] for the fabrication of composites. In our method, the stirring-squeeze casting method techniques was used. The squeeze casting methods provide less porosity due to the elimination of gases; during the pressing process, desired surface texture, expected microstructures and less wastage with more strength of the casting composites could be achieved.[11] The technical challenges are that the need of great attention for: achieving homogeneous distribution of reinforcements in the MMCs. The wettability of the particles in the matrix, porosity developed from casting and chemical interaction between matrix and the reinforcements are the main parameters.[11–13] This problem is common to most production routes, including stirring-squeeze casting. To achieve the desired properties, these problems must be optimized. The method of supersonic vibration removes the gas formation during the process of fabrication and reduces the level of porosity in the cast.[14] In a quasi-crystalline state, the preservation of Cu–Cr–Fe particles in the Al7075 composites formed the strong mechanical interlocking with the Al matrix. Li et al studied the effect of incorporation of these particles into the Al matrix and concluded a significant improvements in the wear resistance and modifications in the mechanisms of wearing.[15] The interface contact and interfacial adhesion between the CNTs and Cu Cr matrix improve the strength and ductility of the composites. Zhao et al., reported that the strengthening behaviour of Al7075 MMCs by CNTs reinforcement.[16] By observing the wear behaviour exhibited by the composites studied by Alaneme et al., there was a considerable increase in wear resistance by adding silicon carbide and rice husk ash as the reinforcements.[17] Even though hybrid AMMCs show better performance on mechanical and tribological behaviour than the pure alloys, still study under various corrosion surroundings to establish their corrosion performance is still lacking.[18] The improved performance on corrosion resistance of aluminium composites was achieved with the reinforcements of sub-micron B_4C particles in the matrix of aluminium alloy[19] However, the effect of B_4C and BN reinforcements on the tribological and corrosion properties of Al7075 MMCs has not been investigated in detail. Moreover, the stirring-squeeze casting process and comparative study on mechanical, tribological and corrosion behaviour of B_4C/BN co-reinforced Al7075 alloy with B_4C-reinforced Al7075 alloy was not reported. Therefore, in the present work, different weight percent of B_4C and constant weight percentages of BN particles have been added to synthesis Al7075/B_4C/BN hybrid composites to analyse the microstructure, mechanical, tribological and corrosion properties for the composites, synthesized through the route of squeeze casting method.

Experimental Methodology

Materials Selection

Zinc-based Al7075 aluminium alloy with copper and magnesium provide the highest strengths compared to any other commercial series of alloys. However, the Al7075 alloys possess relatively poor corrosion resistance compared to other aluminium alloys. Therefore, it is highly imperative to improve the corrosion resistance of Al7075 to widen its applications in the marine environment and further improve mechanical behaviour for the automobile industry applications.[20] Hence, in the present work, Al7075 alloy has been chosen as the base matrix to improve mechanical, tribological and anticorrosion properties by reinforcing with B_4C and BN particles. The constituents of the base matrix are specified in Table 1.

Density is the most important factor for selecting reinforcement particles. Priority should be given to the low-

Table 1. Constituents of Al7075 Aluminium Alloy

Concentration wt%								
Cr	Cu	Fe	Mg	Mn	Si	Ti	Zn	Al
0.28	2.0	0.5	2.6	0.3	0.4	0.2	5.8	Balance

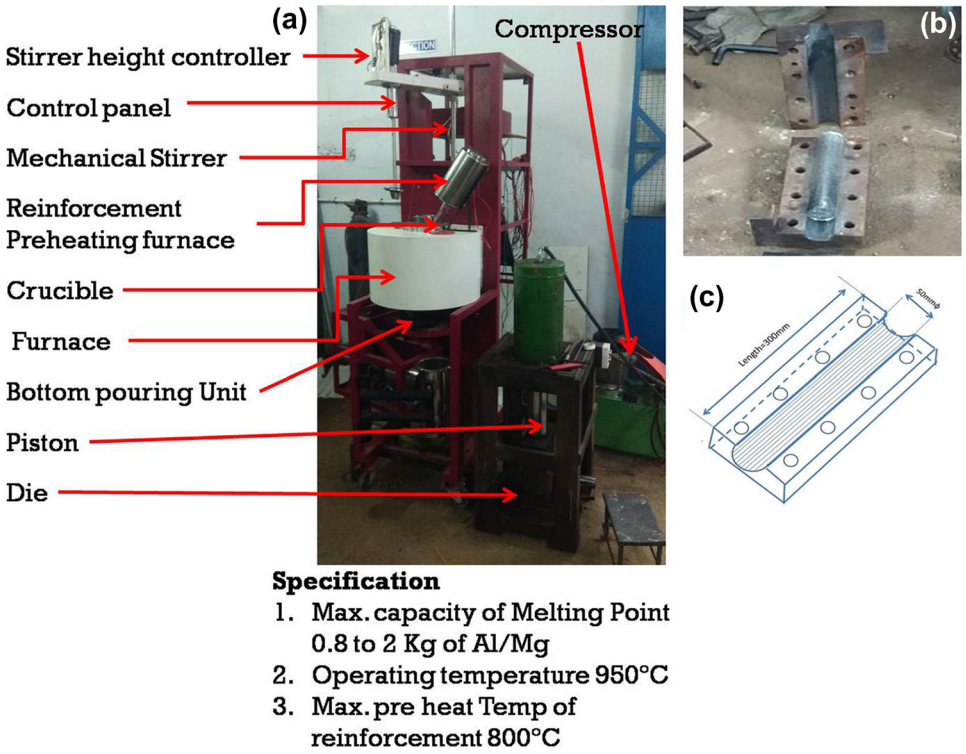

Figure 1. (a) Image of squeeze casting setup, (b) image of die used for casting with casted specimen, c the dimensional sketch of die used.

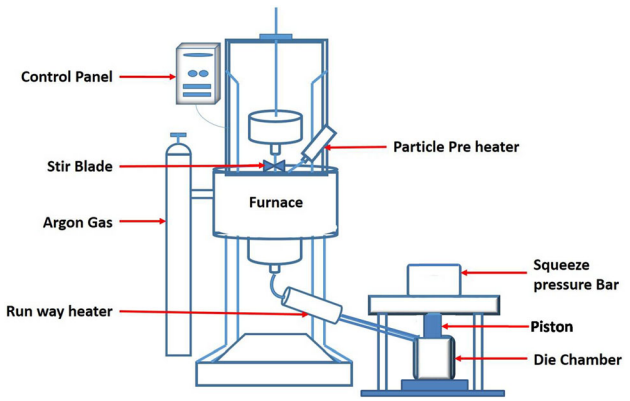

Figure 2. Schematic diagram of the fabrication process.

density material in weight-sensitive sectors such as the automotive and marine applications. In the present work, 1-μm size B_4C and 10-micron size BN particles have been selected as reinforcement particles with densities of 2.5 g/cm^3 and 2.1 g/cm^3, respectively, which are relatively less than that of Al7075 alloy (2.8 g/cm^3). Since the reinforcements are of lower density than the base matrix, by the law of mixtures the overall density of the hybrid composites will be less than that of the base matrix. From the literature study, it is observed that the weight percentages of reinforcement for aluminium matrix composite are mostly kept at below 10% with very few experiments exceeding 10%.[21,22] In the present study, three aluminium metal matrix composites (AMMCs) and three aluminium hybrid metal matrix composites (AHMMCs) have been prepared with compositions (Al7075 + x%B_4C) and (Al7075 + x%B_4C + 3%BN) where x = 3, 6, 9 (measured in wt.%). Since B_4C is a harder substance, exhibits desired wettability, good thermal stability and exceptional chemical inertness, it is chosen to be primarily used as reinforcement in aluminium composites.[21] Properties of BN such as lamellar crystal structure, good lubrication, high thermal conduction, low thermal expansion, superior shock resistance and excellent workability[23] make it a good

Table 2. Manufactured AMMCs and AHMMCs and Its Compositions

Sl. no.	Testing materials	Weight percentage		
		Al7075	B_4C	BN
1.	Al7075	100	–	–
2.	Al7075/3%B_4C(AMMC1)	97	3	–
3.	Al7075/6%B_4C (AMMC2)	94	6	–
4.	Al7075/9%B_4C(AMMC3)	91	9	–
5.	Al7075/3%B_4C / 3%BN(AHMMC1)	94	3	3
6.	Al7075/6%B_4C / 3%BN(AHMMC2)	91	6	3
7.	Al7075/9%B_4C / 3%BN(AHMMC3)	88	9	3

reinforcement for the usage in high temperature and high wear applications. BN forms stable chemical bonds with aluminium resulting in a uniform and stable microstructure. Thus, BN is selected as secondary reinforcement with a fixed weight percentage of 3%.

Stirring-Squeeze Casting Processes

The stirring-squeeze casting method can provide a significant interface between reinforcements and is thereby well suited for fabricating hybrid composites.[11] In the present work, the pure and hybrid composites of Al7075 alloy were prepared by the conventional stir casting method using a resistive heating furnace (graphite crucible) with an impeller. Approx. 1/3 of melt height has been maintained to the bottom of the crucible. Initially, the alloy was melted at the temperature of 700 °C. Further, the temperature was raised to 750 °C and maintained for 20 min to ensure a homogeneous melt. The melting process was carried out in an inert atmosphere containing a continuous flow of the mixture of Argon and SF6 at the rate of 3.5 l/min to limit the reaction between MMC and air. The preheated B_4C and BN reinforcements particles were gravity fed into the molten alloy. The stirring is started and then reinforcements were added. Particles entered into the vortex created by the stirring in the melt and the temperature was further increased to 850 °C. Stirring of the melt was carried out at the speed of 500 RPM for 15 min to obtain a homogeneous mixture. The particles distribution may be affected by several factors like rheological behaviour, the method of incorporation of particles, interactions, distribution during solidifications and density of matrix and particles.[24] Thus, careful attention has been given to the above factors. The particles with respective concentrations were added to the molten matrix. Since at relatively lower temperature B_4C particles exhibit lower wettability with molten aluminium matrix,[25,26] the temperature and stirring speed further increased to 950 °C and 600 RPM, and this state was maintained for 20 min. To avoid rapid cooling of the composite while casting, a pressure of 100 MPa was maintained at each pressing and this pressure level is maintained till the end of the process of solidification. The graphite coated die temperature was maintained at 250 °C. The molten matrix has been poured into it and allowed to cool under ambient temperature after being punched by hydraulic press. The same procedures have been repeated for all composites. Figure 1 shows the (a) image of squeeze casting setup (b) image of die used for casting with casted specimen (c) the dimensional sketch of die used. Figure 2 shows the schematic diagram of the fabrication process.

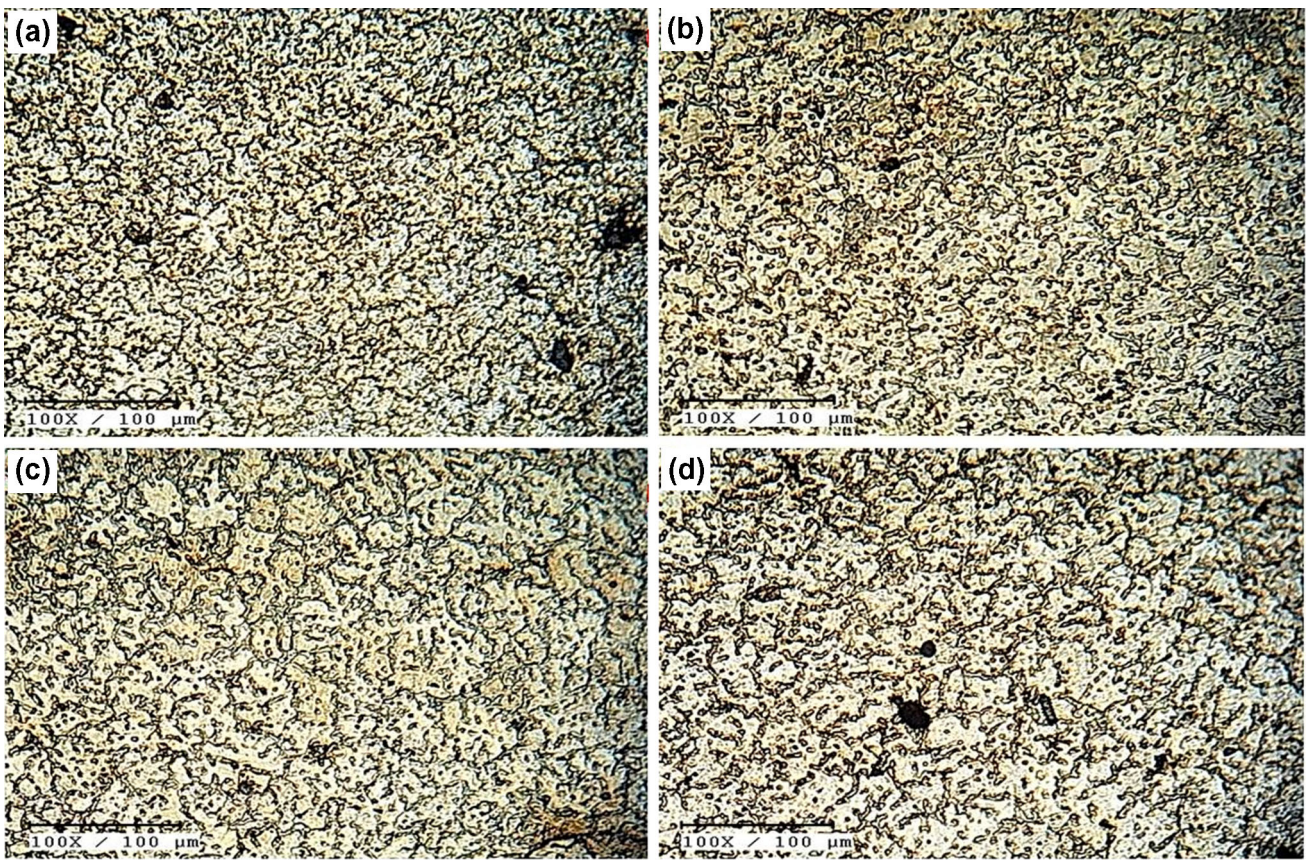

Figure 3. Microstructure of (a) Al7075, (b) AHMMC1, (c) AHMMC2 and (d) AHMMC3 at etched conditions.

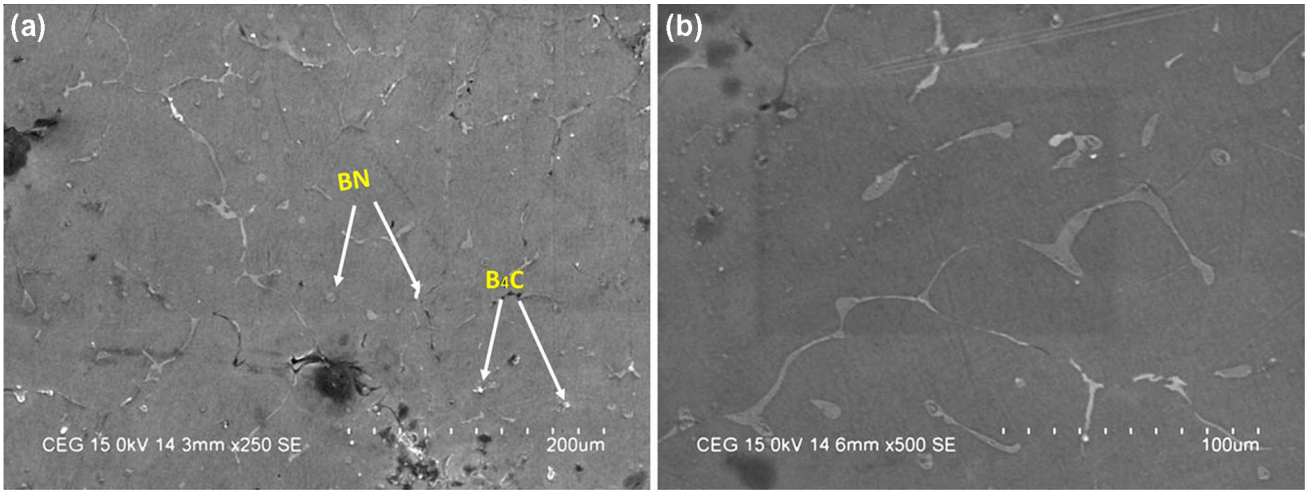

Figure 4. SEM image of (a) AHMMC2, (b) AHMMC3.

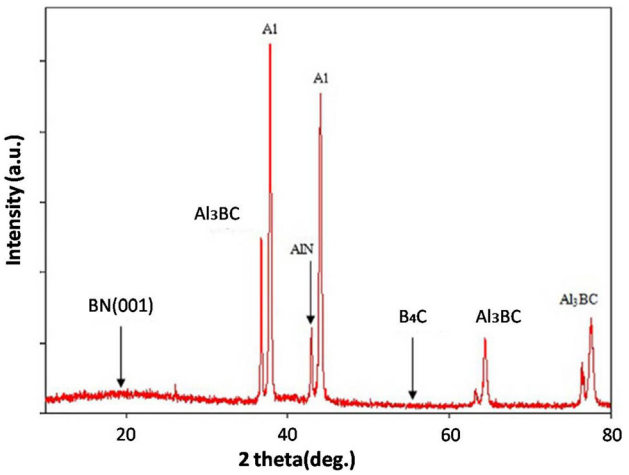

Figure 5. XRD patterns of AHMMCs.

The synthesized AMMCs and HAMMCs and their compositions are shown in Table 2

Measurement of Properties

The microstructure analysis of prepared hybrid composites has been performed using an optical microscope. The distribution of reinforcement particles has been confirmed by SEM analysis. The micro-hardness of the hybrid composites was studied by Vickers micro-hardness tester. The specimens with the dimensions of 32 mm length, 6 mm width and 3.5 mm thickness were prepared as per the standard of ASTM E-8 for the tensile test. To minimize the error, an interpolation technique was adapted through averaging of tested values of five specimens. The prepared specimens were subjected to a compression test as per ASTM E9 standard. The specimen's dimensions for the compression test were 10 mm in diameter and length of 25 mm. Salt spray test has been carried out as per the ASTM B-117 standard on the composites and unreinforced alloy to study the anticorrosion properties of composites. Rectangular samples of 25 × 25 mm and 3.5 mm thickness were prepared for all the hybrid composites to conduct salt spray tests. The prepared samples were pre-polished and pre-cleaned before the test. Pin on disc wear testing machine was used to study the wear properties of synthesized hybrid aluminium composites under dry sliding conditions as per ASTM G99-04. The steel material EN31 of surface roughness 0.3 μm was used as a complement of rotating disc. The wear specimens have been prepared with 8 mm diameter, 32 mm length and spherical end nose radius of 4 mm. The wear track width at the composite contact surface was measured using a universal measuring microscope. The volume of wear loss was calculated as per ASTM G77-83. The effect of formation of the intermetallic phase on microstructure, hardness, tensile strength, compressive strength and the corrosion resistance of hybrid composites has been investigated, and the experimental results have been comparatively discussed with the Al/B_4C composites and base alloy.

Salt spray test was conducted on the prepared composites as per ASTM B117 standards. This test was conducted in a controlled corrosion environment and the result of corrosion resistance value for the composite specimens in the given test chamber was recorded. One side of the specimens was polished using SiC 1200 grade sheet. Marking is done on the unpolished side of the specimens and the initial weight of each composites specimen was recorded using a weigh balance of accuracy 0.001 g. Then the specimens were exposed to a chamber for salt spray test and were positioned at an angle of 25° to the vertical. The periodical salt spray was done especially on the polished side for a period of 1.5 h then off period of 1.5 h, for 2 days. The 3.5 wt% of salt solution was employed for the wetting cycle and the chamber temperature was maintained at 25 °C.[18] Two specimens for each composite were taken for corrosion tests.

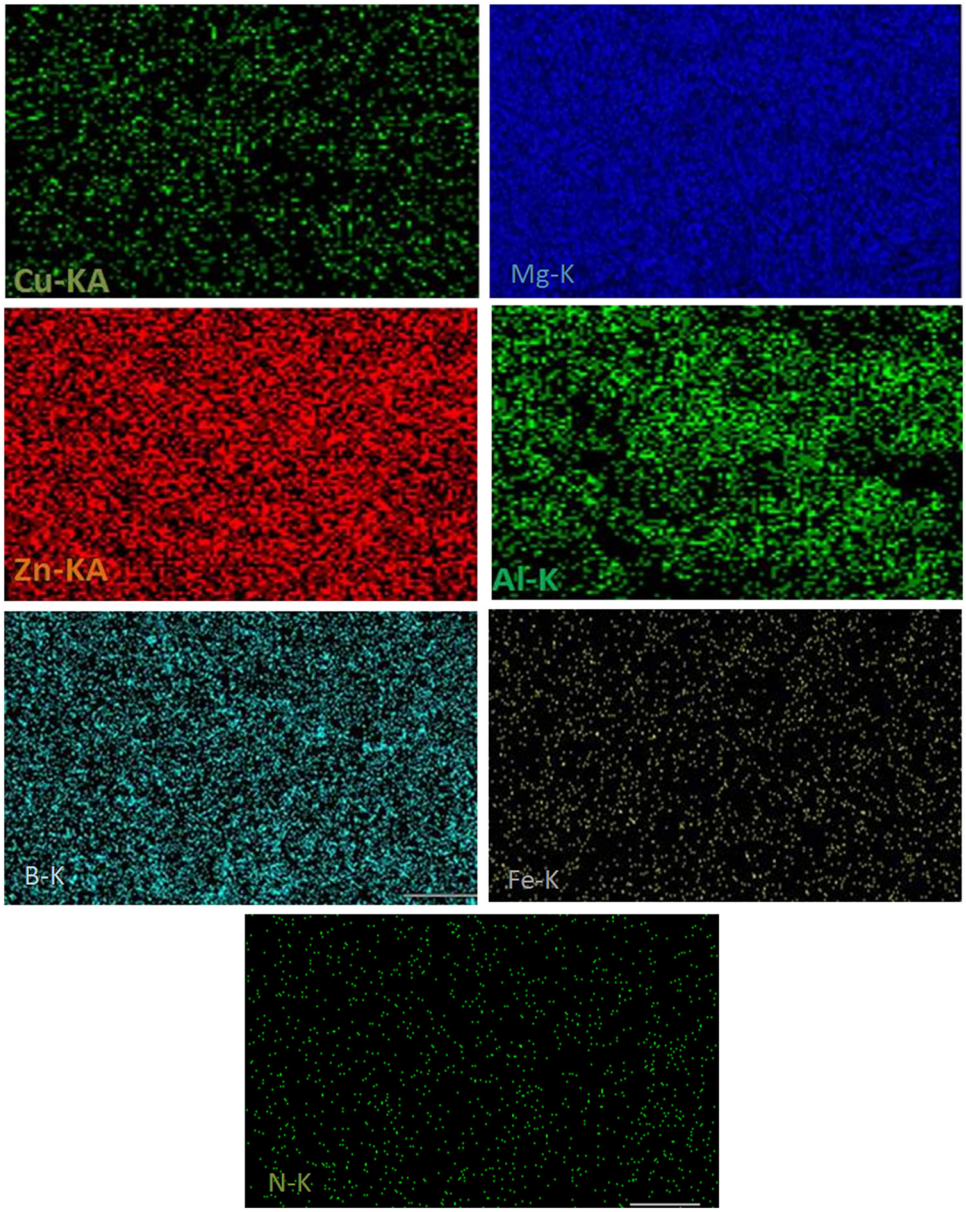

Figure 6. Elements presents of AHMMCs.

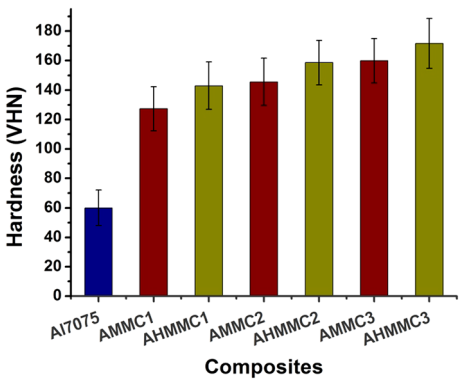

Figure 7. Vickers hardness of AA7075, AMMCs and AHMMCs.

Table 3. Tensile Strength, Yield Strength and % of Elongation of AA7075, AMMCs and AHMMCs

Specimen name	Densities (g/cm^3)	Tensile strength in N/mm^2	Yield strength in N/mm^2	% of Elongation
Al7075	2.800	221±11	95±5	6.20±1.5
AMMC1	2.791	286±10	144±5	2.57±0.6
AMMC2	2.782	296±9	162±6	1.94±0.2
AMMC3	2.773	313±12	171±7	1.53±0.3
AHMMC1	2.77	322±8	167±6	2.28±0.7
AHMMC2	2.761	355±9	183±6	1.67±0.3
AHMMC3	2.752	368±7	199±7	1.38±0.4

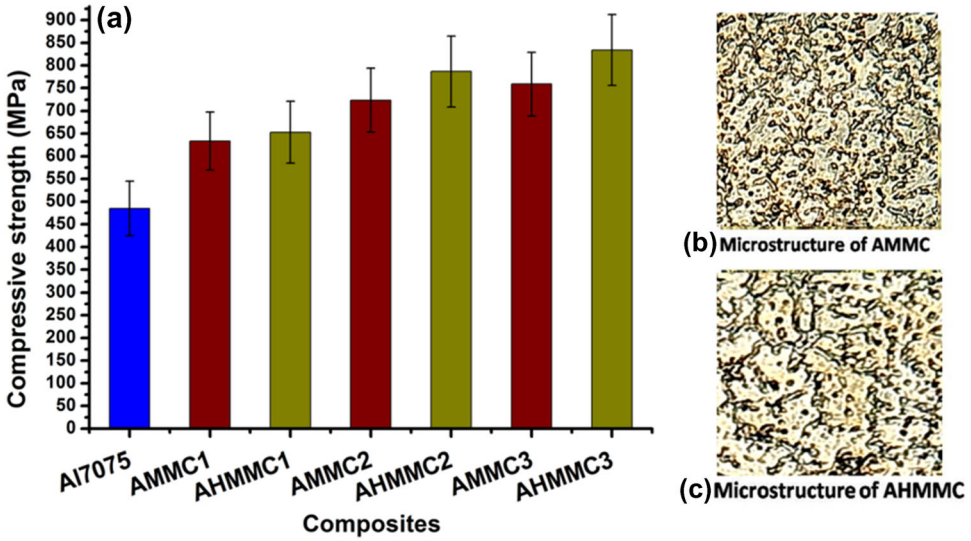

Figure 8. Compressive strength of AA7075 alloy, AMMCs and AHMMCs.

Results and Discussion

Structural Analysis

Microstructure Analysis

Studies on microstructure were conducted for all composites with the help of an optical microscope on the specimens' etched surface. The dark-colour intermetallic phases like Al_3BC, AlB_{12} and AlN are shown in the bright metal matrix for all samples. However, due to the squeeze casting a greater number of grains are observed in the microstructure. As can be seen from Figure 3a for Al7075 alloy, relatively smaller grain sizes (10–15 μm) than the AHMMC 1, 2 and 3 as shown in Figure 3b–d (18–23 μm, 23–25 μm and 24–35 μm). Moreover, the increasing the % of reinforcements or increasing the volume of intermetallic phases lead to increasing size of the grains in the AHMMC3. The formation of dendrite pattern by the fine grains due to the deposition and precipitation at the intersection of grain boundaries as well as the elevated temperature does not affect the homogeneity of materials as shown in Figure 3. Increasing the area of intermetallic phases in the grain boundaries are improving the performance of the AHMMCs. Both reinforcement particles have been placed in boundaries and lead to a thicker one in the AHMMCs.

SEM Analysis

SEM images for the 6% and 9% B_4C added reinforced hybrid composites are shown in Figure 4. It has been observed that the reinforcing particles (B_4C and BN) are embedded in the MMCs as the particles are observed in the SEM images of synthesized hybrid aluminium composites. In general, the reinforcement particles have higher hardness and have higher melting points than a matrix material. A needle-shaped formation of Al_3BC, AlB_{12} and AlN particles precipitated in the grain boundaries of the composites. The dispersion of reinforcement particles prevents the motion due to dislocation and improves the strength of materials which gives the better behaviour on the mechanical and corrosion properties. The enhancement of compressive strength is due to the dispersed reinforcement particles in the matrix, which significantly play an important role in the cushioning effect improvements.

XRD and EPMA Analysis

Figure 5 shows the B_4C and BN particles XRD patterns with varying weight percentages of B_4C (3, 6, and 9%). The XRD patterns confirm the dominant effect of Al in the hybrid composites with high crystalline as the aluminium-related peaks are very sharp and high intensity. In addition, the secondary phases of Al_3BC, AlB_{12}, and AlN are observed in the composites. Owing to the interfacial reaction of reinforcements with aluminium, the secondary phases are formed in the hybrid composite. Such kind of interfacial reaction improves the mechanical properties of composites.[27] The element of pure aluminium alloy and the presents of B_4C and BN reinforcements in the hybrid composites are shown in Figure 6.

Mechanical Properties

Hardness of Alloy and Composites

The two different ceramic reinforcements B_4C and BN having higher hardness than Al7075 alloy contributes to enhancement in the hardness of synthesized hybrid composites. Figure 7 shows the comparison of the hardness of

Table 4. Comparative Investigation of Hybrid Composites Mechanical Behaviours

Composites	% of reinforcement	Processing Technique	Hardness	Tensile	Compression	References
Al/WC/Gr	5 and 10 wt% of WC 4 wt% of Gr Bal AA5052	Melt-stir casting	10.3% and 34.2% increased VHN	15.12% increased	–	30
Al/SiC/Gr	5 and 10 wt% of SiC, 4 wt% of Gr Bal AA5052	Melt-stir casting	2.56% drop VHN	22.88% drop	–	30
Al/B_4C/MoS_2	Al7075 Al7075+4%B_4C+3%MoS_2 Al7075+8%B_4C+3%MoS_2 Al7075+12%B_4C+3%MoS_2	Stir casting	60 VHN 72.5 VHN 88.6 VHN 94.32 VHN	221 N/mm2 268.21 N/mm2 281.32 N/mm2 298.52 N/mm2	–	31
Al/B_4C/CDA (CDA—Cow Dung Ash)	Al7075 Al7075+10%CDA Al7075+2.5%B_4C+7.5%CDA Al7075+5%B_4C+5%CDA Al7075+7.5%B_4C+2.5CDA Al7075+10%B_4C	Two-stage stir casting	110 BHN 103 BHN 119 BHN 132 BHN 144 BHN 152 BHN	188 Mpa 230 Mpa 250 Mpa 268 Mpa 290 Mpa 274 Mpa	–	32
Al/$Y_2W_3O_{12}$/AlN	Al+30%$Y_2W_3O_{12}$ Al+30%$Y_2W_3O_{12}$+5%AlN Al+30%$Y_2W_3O_{12}$+10%AlN Al+30%$Y_2W_3O_{12}$+15%AlN Al+30%AlN Al+5%$Y_2W_3O_{12}$+30%AlN Al+10%$Y_2W_3O_{12}$+30%AlN Al+15%$Y_2W_3O_{12}$+30%AlN	Solid-state powder metallurgy route	75 HV 110 HV 165 HV 230 HV 280 HV 310 HV 325 HV 335 HV	–	290 Mpa 390 Mpa 440 Mpa 500 Mpa 650 Mpa 570 Mpa 540 Mpa 510 Mpa	33
Al/Al_2O_3/SiC/REP (REP—rare earth particulate—CeO_2)	Al6061 Al6061+2.5%Al_2O_3+2.5%SiC Al6061+5%Al_2O_3+5%SiC Al6061+7.5%Al_2O_3+7.5%SiC Al6061+2.5%Al_2O_3+2.5%SiC+0.5%REP Al6061+5%Al_2O_3+5%SiC+1.5%REP Al6061+7.5%Al_2O_3+7.5%SiC+2.5%REP	Stir casting route	79.3 HV 84.8 HV 85.5 HV 90.17 HV 85.67 HV 88.17 HV 92.8 HV	– 30 Mpa 54 Mpa 73 Mpa 89 Mpa 102 Mpa 123 Mpa		34
Al/SiC/ZrO_2	Al7075 Al7075+2%SiC+3%ZrO_2 Al7075+4%SiC+3%ZrO_2 Al7075+6%SiC+3%ZrO_2	Stir casting	89.9 BHN 96 BHN 116.43 BHN 143.64 BHN	115.54 Mpa 118.66 Mpa 121.78 Mpa 131.15 Mpa	43.8 Mpa 47 Mpa 49.8 Mpa 52.8 Mpa	35

Table 4 continued

Composites	% of reinforcement	Processing Technique	Hardness	Tensile	Compression	References
Al/CNT/TiC	Al3003	Stir casting	55 HV	–	–	36
	Al3003+0.5%CNT+0.5%TiC		62 HV			
	Al3003+0.5%CNT+1%TiC		65 HV			
	Al3003+0.5%CNT+1.5%TiC		70 HV			
	Al3003+0.5%CNT+2%TiC		72 HV			
Al/SiC/Gr	Al	Liquid processing technique agitated casting	40 BHN	219 Mpa	–	37
	Al+2%Gr		41 BHN	215 Mpa		
	Al+3%SiC+2%Gr		46 BHN	226 Mpa		
	Al+6%SiC+2%Gr		50 BHN	235 Mpa		
Al/SiC/ZrO_2	Al6061	Stir casting	58 BHN	308 Mpa	194 Mpa	38
	Al6061+2%SiC+3%ZrO_2		68 BHN	345 Mpa	217 Mpa	
	Al6061+4%SiC+3%ZrO_2		80 BHN	368 Mpa	240 Mpa	
	Al6061+6%SiC+3%ZrO_2		95 BHN	382 Mpa	255 Mpa	
Al/TiC/WC	Al6082	Stir casting	53 BHN	146 Mpa	–	39
	Al6082+3%(TiC+WC)		61 BHN	154 Mpa		
	Al6082+6%(TiC+WC)		68 BHN	167 Mpa		
	Al6082+9%(TiC+WC)		75 BHN	178 Mpa		
	Al6082+12%(TiC+WC)		83 BHN	182 Mpa		
Al/TiC/Al_2O_3/Si_3N_4	Al2519+3%TiC+3%Al_2O_3+3%Si_3N_4	Stir-squeeze casting	89.22 HV	174 Mpa	–	11
Al/SiC/FA	A356	–	–	255 Mpa	245 Mpa	40
	A356+5%SiC+10%FA	Stir casting	30% increased	331.5 Mpa	318.5 Mpa	
	A356+5%SiC+10%FA	Stir–squeeze casting	65% increased	408 Mpa	392 Mpa	
Al/B_4C/BN	Al7075	Stir-squeeze casting	60 VHN	221 Mpa	485 Mpa	[Self]
	Al7075+3%B_4C		127.4 VHN	286 Mpa	633.6 Mpa	
	Al7075+6%B_4C		145.6 VHN	296 Mpa	723.8 Mpa	
	Al7075+9%B_4C		159.9 VHN	313 Mpa	759 Mpa	
	Al7075+3%B_4C+3%BN		143 VHN	322 Mpa	653.28 Mpa	
	Al7075+6%B_4C+3%BN		158.6 VHN	355 Mpa	786.77 Mpa	
	Al7075+9%B_4C+3%BN		171.6 VHN	368 Mpa	833.96 Mpa	

alloy and composites. The AMMCs exhibited relatively high hardness compared to the AHMMCs and AAl7075. Furthermore, the hardness of the AMMCs increased with the percentage of B_4C reinforcements. The higher hardness is due to the resistance to the motion of dislocation in the composites than the monolithic alloy.[17] The uniform distribution and the intermetallic phase like $A_{l3}BC$, AlB_{12} and AlN and grain enrichments are the factors for improving the hardness of composites.[28]

Tensile Strength of AA7075, AMMCs and AHMMCs

It is observed that the tensile and yield strength of MMC's and AHMMCs have been increased with the increasing percentage of B_4C particles when compared with the monolithic Al7075 alloy as shown in Table 3. Moreover, the tensile strength of AHMMCs is superior to AMMCs. This is owing to the formation of interfacial reaction, fine grain size, and strengthening effect of strain gradient of BN particles.[29] The increasing percentage of reinforcements in the matrix alloy is reducing the percentage of elongation in the hybrid composites.[17]

Table 5. Wear Track and Wear Rate of AA7075, AMMCs and AHMMCs.

Velocity (m/s)	Load (N)	Wear track width/mm							Wear rate in mm^3/m						
		AA7075	AMMC1	AMMC2	AMMC3	AHMMC1	AHMMC2	AHMMC3	AA7075	AMMC1	AMMC2	AMMC3	AHMMC1	AHMMC2	AHMMC3
0.25	10	2.22	3.44	3.66	3.87	3.09	3.28	3.48	2.30	2.20	2.15	1.89	1.78	1.68	1.58
	20	2.76	4.17	4.25	4.36	3.83	3.88	3.98	2.90	2.50	2.22	1.95	2.58	2.49	2.38
	30	3.01	4.45	4.96	5.30	3.98	4.09	4.28	3.82	3.61	2.94	2.32	3.29	2.92	2.74
0.5	10	2.62	3.89	4.22	4.90	3.59	3.87	3.98	2.50	1.60	1.30	1.11	1.88	1.48	1.39
	20	3.39	4.68	5.23	5.70	4.18	4.61	4.68	3.32	2.43	2.26	2.00	2.81	2.64	2.49
	30	4.09	4.93	5.60	5.79	4.53	4.88	4.97	4.10	3.34	2.90	2.28	3.72	2.88	2.57
1	10	3.09	5.59	5.19	5.80	3.89	3.98	5.07	2.74	2.19	1.83	1.00	1.97	1.91	1.82
	20	3.71	5.63	5.74	6.30	4.71	4.92	5.28	3.84	2.20	1.74	1.29	2.88	2.72	2.59
	30	4.00	5.69	6.40	7.76	4.89	5.08	5.74	4.82	3.34	2.94	2.11	3.93	2.94	2.70

The presents of nucleation sites in the aluminium matrix lead to the composites' recrystallization owing to the forming of grains with the least sizes and this provides a resisting mechanism for the dislocation movements and provides the comprehensive strength of composites. The properties of the brittle nature of reinforced are playing a dominant role decreasing in the ductility of composites and increasing the % of reinforcements control the flowability of the matrix and thus % of elongation of composites are reduced.[28]

Compressive Strength of AA7075, AMMCs and AHMMCs

The Compressive strength exhibited by the composites and the unreinforced alloy is shown in Figure 8a. A significant increase in the compressive strength is observed in the composite with the increase of B_4C content and this can be attributed to the increasing area of interface boundaries between B_4C and Al as B_4C particle concentration in the composite. It is observed that the co-reinforcement of BN further increases the compressive strength of the composites. The homogeneous distribution of B_4C and BN and their strengthening effect support to the composites against compression load. Whereas, raise in % of B_4C would be increasing the strength of interface due to the piling of displacement between boundaries and interfaces. The grain enrichments offered by squeezing and regular geometrical shape of grains (Figure 8b, c) are the influencing factors for the cushioning effect against compressive load.[11] Especially, BN particles in the hybrid composites accelerating for more intermetallic phases as shown in Figure 8c and the improved mechanical properties of synthesized AHMMCs are confirmed through the comparative investigations of various Al hybrid composites as shown in Table 4.

Wear Properties of AA7075, AMMCs and AHMMCs

The wear track width at the composite contact surface was used to measure the wear parameter using a universal measuring microscope. The wear track width and calculated wear rate of synthesized aluminium hybrid composites at dry sliding conditions of varying sliding speeds and applied loads are shown in Table 5. The wear rate of AMMCs has been significantly improved for all the combinations sliding speeds and applied loads. This is due to the increase in load tends to increase the width of synthesized composites and hence the wear rate also increases. Normally the wear rate and wear width of composites are increasing with increasing applied load and speed. Whereas, the wear width and wear rate of the composites were significantly reduced for the same load and same speed for the hybrid composites. Increasing the

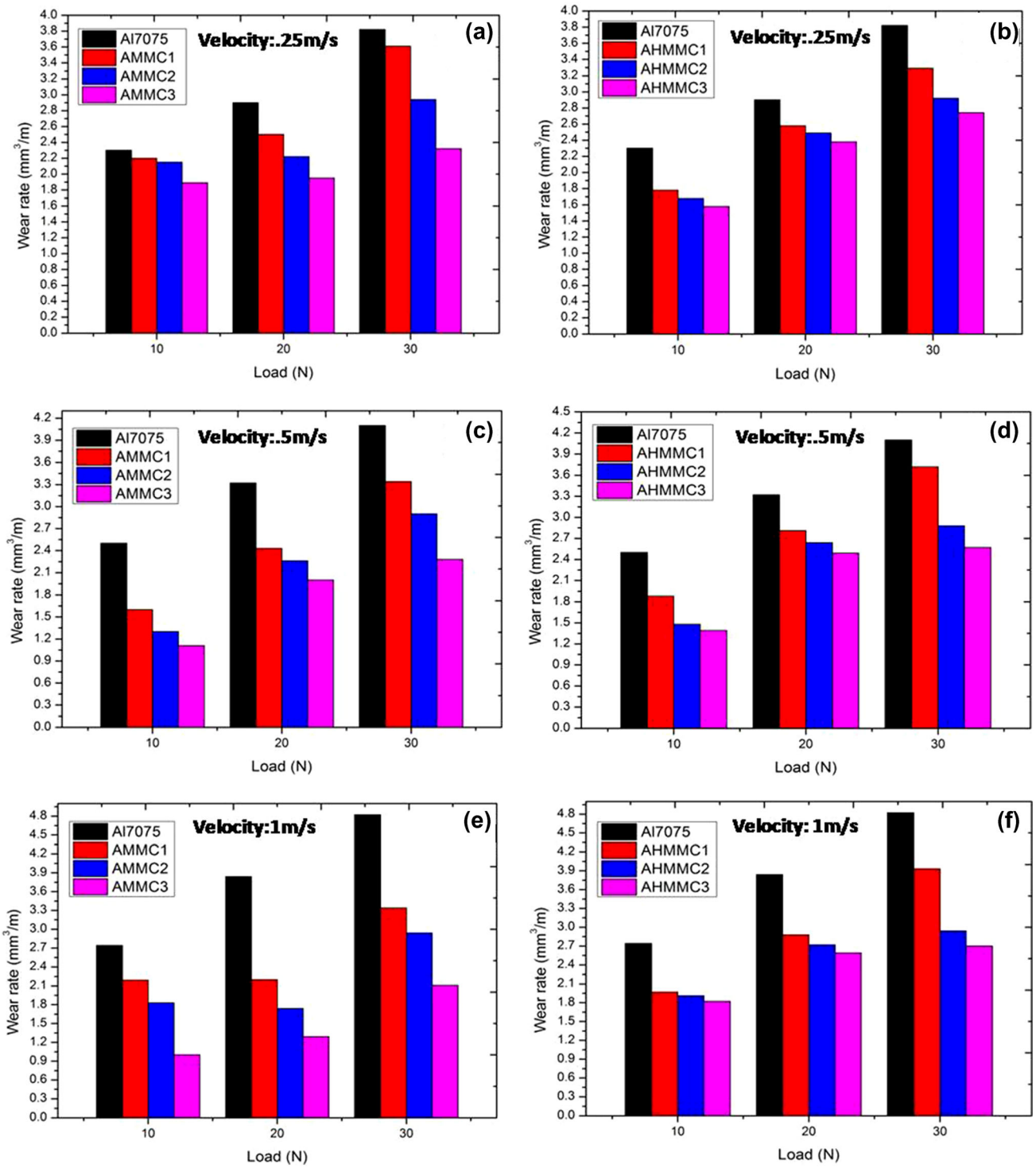

Figure 9. Wear rate of AMMCs (a, c, d) and AHMMCs (b, d, f) specimens for the respective sliding velocities of 0.25m/s, 0.5m/s and 1m/s for the normal load of 10 N, 20 N and 30 N.

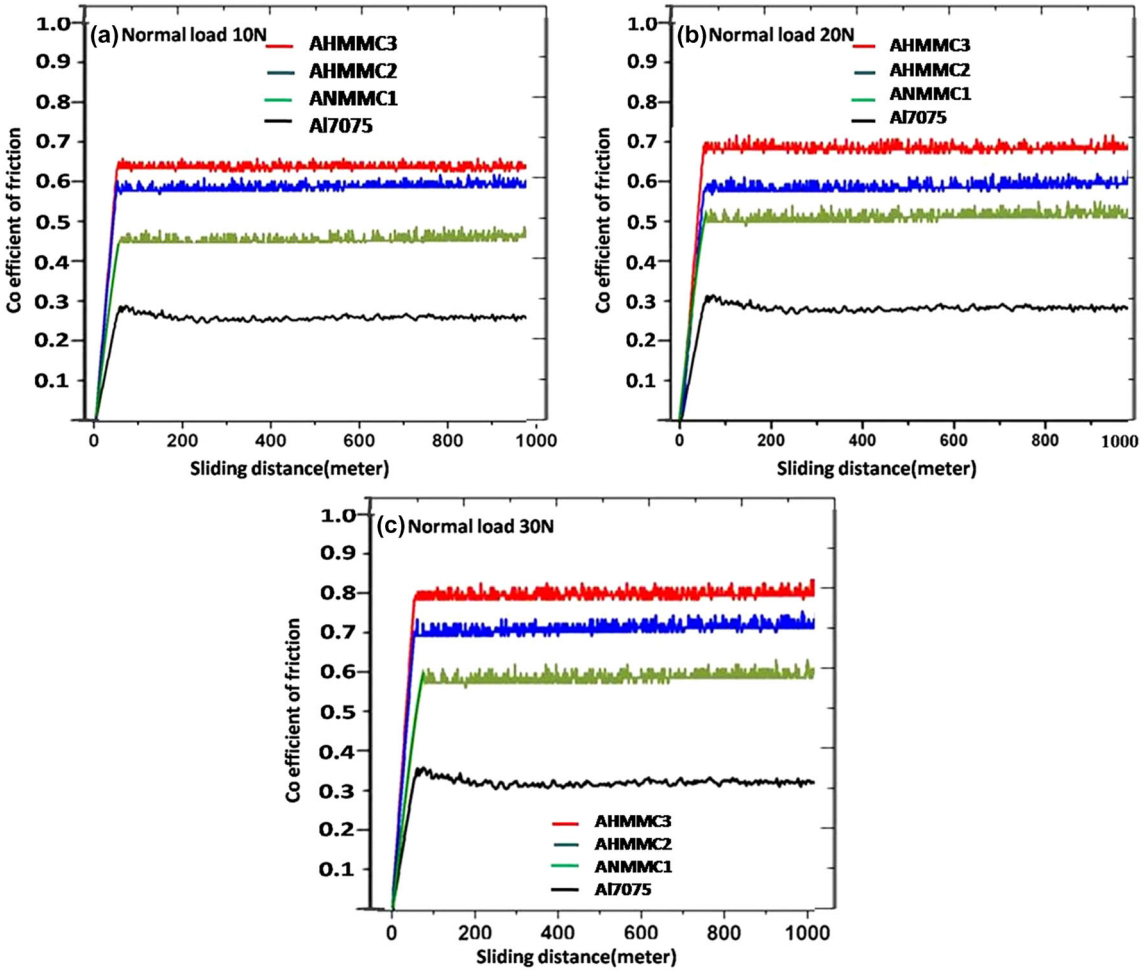

Figure 10. Coefficient of friction of aluminium hybrid composites under varying its weight percentage.

% of B_4C is decreased the wear rate. The presence of stiffer and stronger reinforcement in the matrix alloy and more grains refinement by squeeze casting is restricting the motion of dislocation movement thus hindering the wear rate. Figure 9 shows the graphical representation of wear rate of AMMCs (Figure 9a, c, d) and AHMMCs (Figure 9b, d, f) specimens for the respective sliding velocities of 0, 25 m/s, 0.5 m/s and 1 m/s for the normal load of 10 N, 20 N and 30 N.

Friction Coefficient

The coefficient of friction (COF) with different velocities (0.25 m/s, 0.50 m/s and 1.0 m/s) under three different loads 10 N, 20 N and 30 N have been shown in Figure 10. The COF of B_4C and BN particles reinforced hybrid composites increased with increasing reinforced particles and the values are 0.45, 0.50 and 0.60 for AHMMC1, 0.58 0.60 and 0.70 for AHMMC2, 0.65, 0.70 and 0.80 for AHMMC3 for the applied loads of 10 N, 20 N and 30 N, respectively. It can be seen that the friction coefficient of the hybrid composites has been significantly increased. This is due to the strengthening effect of matrix and reinforcements, the dislocations in the alloy are ineffective which causes the increase in hardness and it is the most important factor to enhance the wear resistance of the reinforced composites.

SEM Study on Wear Out Surfaces of the AMMCs and AHMMCs

Figure 11a–f reveals that the images of worn-out surfaces of the composite specimens for load 30 N. The SEM images of plastic deformation and the presence of grooves parallel with the sliding directions. The furrows and grooves are the typical topographic accompanying abrasive and adhesive wear. Other than grooving, local plastic distortion and particles of material spreading were shown and which indicates abrasive wear. For all the applied load, the wear surface of the AHMMCs specimen (Figure 9a) is smoother than AMMCs (Figure 11d) and shows fine grooves with smaller steps and a plastic stream. Moreover,

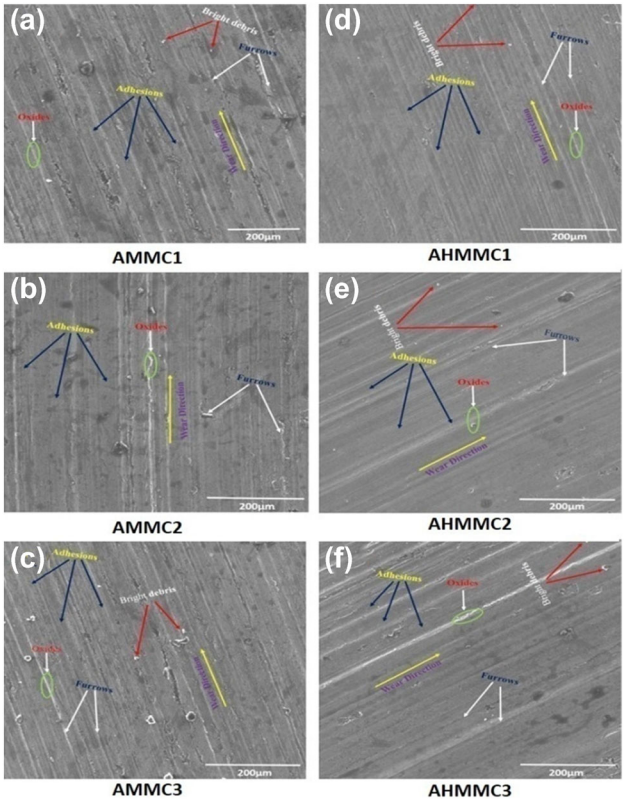

Figure 11. SEM images of AMMCs (a–c) and AHMMCs (d–f) worn-out surface at 1m/s and 30N load.

Table 6. Corrosion Behaviour of AA7075, AMMCs and AHMMCs

Specimen name	Initial weight in g	Final weight in g (after 48 h)	Difference in weight (g)	Corrosion rate (mm/year)
AA7075	5.922	5.202	0.720	0.11213
AMMC1	5.874	5.862	0.012	0.00200
AMMC2	5.876	5.866	0.010	0.00167
AMMC3	5.750	5.741	0.009	0.00150
AHMMC1	5.996	5.989	0.007	0.00117
AHMMC2	5.876	5.870	0.006	0.00100
AHMMC3	5.987	5.983	0.004	0.00067

the stiffer and stronger reinforcements restrict the motion of dislocation movement and hinder the wear rate. BN inclusion leads to less shear stress on the composite and lesser detached particles on the wear process and is beneficial due to self-lubrication properties. This improvement continues for all loads and all composites. As significance, the wear resistivity of the B_4C- and BN-reinforced particles was increased due to the load-bearing capacity of the particles and the creation of transfer layers that shield the surface from abrasion. As the load increases from 10 to 30 N, the morphology of worn-out surfaces of AMMCs (Figure 11a–c) and the AHMMCs (Figure 11d–f) gradually become rougher. Moreover, the adhesive zones have become more, especially for the hybrid composites. The worn-out surface observation suggests that the dominant wear mechanism for all three specimens is particulates micro-fracture. BN particles suppress the wear due to the formation of debris and thus the portion with adhesive wear is larger, thereby the worn-out surface is comparatively smoother in hybrid composites.

Corrosion Properties

Corrosion Rate of AA7075, AMMCs and AHMMCs

The salt spray corrosion test was carried out on the unreinforced aluminium alloy and composites as per ASTM B117 standard. Observed results of unreinforced aluminium alloy and each composite are recorded and presented in Table 6. Aluminium alloys are generally treated as a more reactive material under a corrosive environment due to their high oxygen affinity.[41] The oxidation reaction reduces the value of Ph. Also, the degradation of the matrix of aluminium spreads all over the cathode. But by incorporating suitable reinforcements in the matrix aluminium like B_4C and BN, the rate of corrosion has been significantly reduced. It is recorded that the increased corrosion resistance of the hybrid composites is achieved by increasing the % of B_4C particles in the synthesized composites. However, the formation of aluminium oxide on the surface acts as a protective layer preventing further corrosion due to its inertness.[42,43] It is observed that the corrosion rate of the composites and hybrid composites is significantly decreased. The intermetallic phases like Al_2Cu act as a reaction barrier and prevent the progression of undesired interfacial reactions.[44,45]

SEM Study of the Corroded Surface of AHMMCs

Figure 12 shows the SEM images of the corroded surface of AHMMCs at different magnification. Corrosion started initially at localized sites, preferentially in both cases on primary and secondary phases. For alloy material, this is visible on the surface while these features are so clear for composites probably due to finer grain size. The localized attack invaded the entire surface with continued exposure to give a general corrosion pattern with several particles remaining on the surface unaffected while the entire matrix was dissolved. The degree of the attack revealed the aggressiveness of the corrosive medium. For alloy, corrosion was initiated at the primary phase. Generally, Al alloys possess' high affinity towards oxygen. Hence, treated as the most reactive material. But it gets its inertness and protectiveness from the aluminium oxide formation on the surface of Al. The presence of metastable portion in

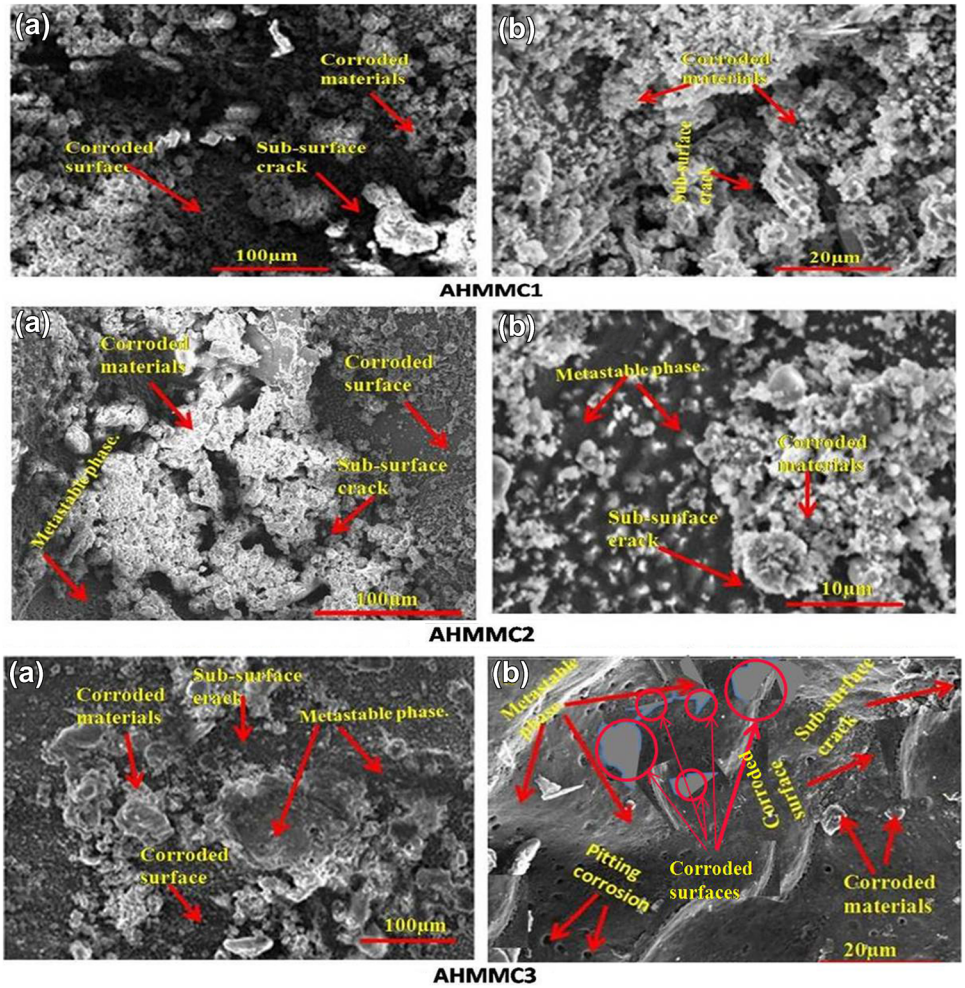

Figure 12. SEM images of the corroded surface of AHMMCs at lower (a) and higher (b) magnifications.

components has been transferred to a great stable region due to the motion of the intermetallic phase. The available composition of composites is the same as the product composition. However, the variation in the structure of atoms on both sides of the interface has occurred. The quality and quality of attack on the surface of the composites show the speed rate of corrosion. Whereas, the increase in the resistance of corrosion due to the increasing % of B_4C can be confirmed through the magnified images of corroded surfaces. An increased rate of corrosion resistance was observed on the surface of the Al7075/9% B_4C/3%BN hybrid composites compared to other hybrid Al composites. Predominantly, the intermetallic phases form the metallization to the fierceness of Cl ions. A Logarithmic increment has been existing between Cl ions and the severity of corrosion. B_4C and BN reinforcement particles provide high diffusivity to the Cl ions to line up the passivation. The formation of the metastable region in the composite material would change to a stable phase through a partition less transformation due to the movement of intermetallic materials in the interface. Moreover, the stable region provided a similar composition of the materials as the existing phase, there could be a difference in the configurations of the atoms on both sides of the interface.

Conclusion

In this study microstructure, mechanical, tribological and corrosion properties of B_4C/BN-reinforced Al7075 hybrid composites have been studied and compared with that of B_4C-reinforced Al7075 composites and Al7075 aluminium alloy.

The following conclusions are made.

1. The AHMMCs with various weight % (3%, 6% and 9% by weight) of B_4C and fixed weight percentage (3%) of BN particulates were synthesized using the stirring-squeeze cast method.
2. The microstructural and SEM studies show the distribution of B_4C, BN particles and sizes of the grains. The formation of intermetallic phases like

Al_3BC, AlB_{12} and AlN were confirmed by XRD. The composition of elements was further confirmed with EPMA test.

3. The hybrid composites (AHMMCs) exhibits improved properties such as hardness, tensile strength, compressive strength, wear resistance, and corrosion resistance compared to Al7075 and the AMMCs.

Abbreviations

μ	Micron
AHMMC	Aluminium hybrid metal matrix composite
Al	Aluminium
Al_2O_3	Aluminium oxide
Al_3BC	Alumino-boron carbide
AlB_{12}	Aluminium dodecaboride
AlN	Aluminium nitride
AMMC	Aluminium metal matrix composite
ASTM	American society of testing and materials
B	Boron
C	Carbon
CNTs	Carbon nanotubes
Cr	Chromium
Cu	Copper
EPMA	Electron probe micro-analysis
Fe	Iron
Gr	Graphite
Hrs	Hours
Li	Lithium
Mg	Magnesium
Mn	Manganese
MPa	Mega pascal
RPM	Revolution per minutes
SEM	Scanning electron microscope
SF6	Sulphur hexafluoride
SiC	Silicon carbide
Si	Silicon
TiB_2	Titanium diboride
TiC	Titanium carbide
Ti	Titanium
VHN	Vickers hardness numbers
wt	Weight
XRD	X-ray diffraction
Zn	Zinc

Acknowledgements

The authors are grateful to Prof. Dr. S. Arunachalam, Founder, ARM College of Engineering and Technology, Maraimalai Nagar, Chennai, for his constant support for the research work. The authors are thankful to Prof. R. Jayavel, Director, Centre for Nanoscience and Technology, Anna University, Chennai, India, for extending the facilities to analyse the samples.

REFERENCES

1. Reddy, P. Venkateshwar, G. Suresh Kumar, D. Mohana Krishnudu, H. Raghavendra Rao (2020). https://doi.org/10.1007/s40735-020-00379-2
2. A. Baradeswaran, S.C. Vettivel, A. Elaya Perumal, N. Selvakumar and R. Franklin Issac, Mater. Des. (2014). https://doi.org/10.1016/j.matdes.2014.06.054
3. G.Kumaresan, B. Arul kumar, Inter Metalcast (2022). https://doi.org/10.1007/s40962-021-00741-1
4. Michael Oluwatosin Bodunrin, Kenneth Kanayo Alaneme and Lesley Heath Chown, J. Mater. Res. Technol. (2015). https://doi.org/10.1016/j.jmrt.2015.05.003
5. S. Johny James, M. Ganesan, P. Santhamoorthy and P. Kuppan, Mater. Today Proc. (2018). https://doi.org/10.1016/j.matpr.2018.02.291
6. Hafeez Ahamed and V. Senthilkumar, Mater. Charact. (2011). https://doi.org/10.1016/j.matchar.2011.10.011
7. Hafeez Ahamed and V. Senthilkumar, Mat. Des. (2012). https://doi.org/10.1016/j.matdes.2011.12.036
8. K. Kanthavel, K.R. Sumesh and P. Saravanakumar, Alexandria Engineering Journal (2016). https://doi.org/10.1016/j.aej.2016.01.024
9. Patidar, Dinesh, R. S. Rana (2017). https://doi.org/10.1016/j.matpr.2017.02.180
10. Fenghong, Cao, Chen Chang, Wang Zhenyu, T. Muthuramalingam, G. Anbuchezhiyan (2019). https://doi.org/10.1007/s12633-018-0051-6
11. T. Adithiyaa, D. Chandramohan, T. Sathish, Mater. Today. Proc. (2020). https://doi.org/10.1016/j.matpr.2019.10.051
12. Suthar, Jigar, K. M. Patel (2018).https://doi.org/10.1080/10426914.2017.1401713
13. Soltani, Shahin, Rasoul Azari Khosroshahi, Reza Taherzadeh Mousavian, Zheng-Yi Jiang, Alireza Fadavi Boostani, Dermot Brabazon (2017). https://doi.org/10.1007/s12598-015-0565-7
14. Vasanthakumar Pandian and Sekar Kannan, Mater. Today Commun. (2021). https://doi.org/10.1016/j.mtcomm.2020.101732
15. F.Z. Li, L.H. Tian, R.T. Li, Y. Wang and Z.Q. Liu, Compos. Interfaces (2019). https://doi.org/10.1080/09276440.2019.1655317
16. Qi Zhao, Xueping Gan, Qian Lei, Wanyu Li and Kechao Zhou, Compos. Interfaces (2020). https://doi.org/10.1080/09276440.2019.1707026
17. Kenneth Kanayo Alaneme, Tolulope Moyosore Adewale and Peter Apata Olubambi, Journal of Materials Research and Technology (2014). https://doi.org/10.1016/j.jmrt.2013.10.008
18. G.R. Gurunagendra, B.R. Raju, Vijayakumar Pujar, D.G. Amith, Poornachandra and H.S. Siddesha, Mater. Today. Proc. (2021). https://doi.org/10.1016/j.matpr.2021.01.892
19. D.M. Shinde, P. Sahoo, Inter Metalcast (2021). https://doi.org/10.1007/s40962-021-00692-7

20. C. Elanchezhian, B. Vijaya Ramnath, G. Ramakrishnan, K.N. Sripada Raghavendra, Mithun Muralidharan and V. Kishore, Mater. Today. Proc. (2018). https://doi.org/10.1016/j.matpr.2017.11.203
21. V. Vignesh Kumar, K. Raja, V. S. Chandra Sekar and T. Ramkumar, Journal of the Brazilian Society of Mechanical Sciences and Engineering (2019). https://doi.org/10.1007/s40430-019-1728-5
22. Rao, PS Raghavendra, C. B. Mohan (2020). https://doi.org/10.1016/j.matpr.2020.03.495
23. K. Srivallirani and M. Venkateswara Rao, Mater. Today. Proc. (2021). https://doi.org/10.1016/j.matpr.2020.06.386
24. Manish Shukla, S.K. Dhakad, Pankaj Agarwal and M.K. Pradhan, Mater. Today. Proc. (2018). https://doi.org/10.1016/j.matpr.2017.12.180
25. Nagaral, Madeva, Shivananda Kalgudi, Virupaxi Auradi, Shivaputrappa Amarappa Kori (2018). https://doi.org/10.1080/0371750X.2018.1506363
26. Massoud Malaki, Alireza Fadaei Tehrani, Behzad Niroumand and Manoj Gupta, Metals (2021). https://doi.org/10.3390/met11071034
27. Guo, Baisong, Min Song, Jianhong Yi, Song Ni, Tao Shen, Yong Du (2017). https://doi.org/10.1016/j.matdes.2017.01.096
28. Esteban Broitman, Tribol. Lett. (2016). https://doi.org/10.1007/s11249-016-0805-5
29. B.N. Sarada, P.L. Srinivasa Murthy and G.Ugrasen, Mater. Today. Proc. (2015). https://doi.org/10.1016/j.matpr.2015.07.305
30. Dhas, DS Ebenezer Jacob, C. Velmurugan, K. Leo Dev Wins, K. P. BoopathiRaja (2019). https://doi.org/10.1016/j.ceramint.2018.09.216
31. Liu, Shoufa, Yinwei Wang, T. Muthuramalingam, G. Anbuchezhiyan (2019). https://doi.org/10.1016/j.compositesb.2019.107329
32. R. Manikandan, T. V. Arjunan (2020). https://doi.org/10.1016/j.compositesb.2019.107668
33. Sethi, Jamuna, Siddhartha Das, Karabi Das (2019). https://doi.org/10.1016/j.jallcom.2018.10.017
34. Sharma, Vipin Kumar, Vinod Kumar, Ravinder Singh Joshi (2019). https://doi.org/10.1016/j.jmrt.2019.06.025
35. Nathan, V. Boobesh, R. Soundararajan, C. Brainard Abraham (2019). https://doi.org/10.1016/j.matpr.2019.07.109
36. Nayim, SM Towhidul Islam, Muhammed Zahid Hasan, Prem Prakash Seth, Pallav Gupta, Sunil Thakur, Devendra Kumar, Anbesh Jamwal (2020). https://doi.org/10.1016/j.matpr.2019.08.203
37. R.S. Rana, Rajesh Purohit (2020). https://doi.org/10.1016/j.matpr.2020.02.650
38. Nathan, V. Boobesh, R. Soundararajan, C. Brainard Abraham, E. Vinoth, J. K. Narayanan (2021). https://doi.org/10.1016/j.matpr.2020.04.643
39. C. Rajaganapathy, D. Vasudevan, A. Dyson Bruno, T. Rajkumar (2021). https://doi.org/10.1016/j.matpr.2020.06.346
40. Ranganathan, Soundararajan, Sathishkumar Kuppuraj, Karthik Soundarrajan, Ashokvarthanan Perumal (2019). https://doi.org/10.4271/2019-28-0113
41. S. Dinesh Kumar, M. Ravichandran, A. Jeevika, B. Stalin, C. Kailasanathan and A. Karthick, Ceram. Int. (2021). https://doi.org/10.1016/j.ceramint.2021.01.158
42. Seun Samuel Owoeye, Davies Oladayo Folorunso, Babatunde Oji and Sunday Gbenga Borisade, J. Adv. Manuf. Technol. (2019). https://doi.org/10.1007/s00170-018-2760-9
43. Min Ao, Huimin Liu, Chaofang Dong, Shan Feng and Juncheng Liu, J. Alloys Compd. (2019). https://doi.org/10.1016/j.jallcom.2020.157838
44. A. Baradeswaran and A. Elaya Perumal, Compos. B. Eng. (2013). https://doi.org/10.1016/j.compositesb.2013.05.012
45. Balasubramani Subramaniam, Balaji Natarajan, Balasubramanian Kaliyaperumal and Samson Jerold Samuel Chelladurai, China Foundry (2018). https://doi.org/10.1007/s41230-018-8105-3